Pervasive and Mobile Computing 10 (2014) 34–50

Contents lists available at ScienceDirect

Pervasive and Mobile Computing

journal homepage: www.elsevier.com/locate/pmc

Sleep posture analysis using a dense pressure sensitive bedsheet

Jason J. Liu [a], Wenyao Xu [b,*], Ming-Chun Huang [a,*], Nabil Alshurafa [a], Majid Sarrafzadeh [a], Nitin Raut [c], Behrooz Yadegar [c]

[a] Wireless Health Institute, University of California, Los Angeles, 90095, United States
[b] Department of Computer Science and Engineering, The State University of New York (SUNY) at Buffalo, NY, 14260, United States
[c] Medisens Wireless Inc., Santa Clara, CA, 95051, United States

ARTICLE INFO

Article history:
Available online 31 October 2013

Keywords:
Sleep posture analysis
Pressure image
Sparse classifier
Image analysis
Bedsheet

ABSTRACT

Sleep posture affects the quality of our sleep and is especially important for such medical conditions as sleep apnea and pressure ulcers. In this paper, we propose a design for a dense pressure-sensitive bedsheet along with an algorithmic framework to recognize and monitor sleeping posture. The bedsheet system uses comfortable textile sensors that produces high-resolution pressure maps. We develop a novel framework for pressure image analysis to monitor sleep postures, including a set of geometrical features for sleep posture characterization and three sparse classifiers for posture recognition. In demonstrating this system, we run 2 pilot studies: one evaluates the performance of our methods with 14 subjects to analyze 6 common postures; the other is a series of overnight studies to verify continuous performance. The experimental results show that our proposed method enables reliable sleep posture recognition and offers better overall performance than traditional methods, achieving up to 83.0% precision and 83.2% recall on average.

Published by Elsevier B.V.

1. Introduction

During the average 7–9 h per day that we sleep, the human body heals itself and grows. Those who have poor sleeping quality are prone to stress, fatigue, attention deficit, or eating disorders [1]. Sleep stage is a proven biometric in diagnosing cardiovascular disease, diabetes and obesity [2]. Sleep difficulty is associated with psychiatric disorders such as depression, alcoholism and bipolar disorder [3].

Among the indicators of determining sleep quality (such as sleep stage and sleep difficulty), *sleep posture* is also one of the most important factors and is heavily used in performing medical diagnoses. One of the most common conditions is sleep apnea. In recent years, several research works on sleep apnea analysis with sleep postures have been investigated. Lee et al. reported that lateral (lying on side) postures can reduce sleep disorders for mild and moderate sleep apnea patients [4]. In related medical conditions, Ambrogio et al. discovered the relationship between sleep postures and chronic respiratory insufficiency, which leads directly to sleep apnea [5]. Further work by Oksenberg and Silverberg investigated breathing disorder and sleep postures [6]. These authors all concluded that patients with respiratory conditions should avoid sleep in the supine (lying on back) position.

In addition to direct effects on respiratory problems, sleep posture can be important during recovery from serious operative procedures. It has been shown that sleep quality affects the recovery times of patients in hospitals [7]. More

* Corresponding authors.
E-mail addresses: wenyaoxu@buffalo.edu (W. Xu), mingchuh@cs.ucla.edu (M.-C. Huang).

1574-1192/$ – see front matter. Published by Elsevier B.V.
http://dx.doi.org/10.1016/j.pmcj.2013.10.008

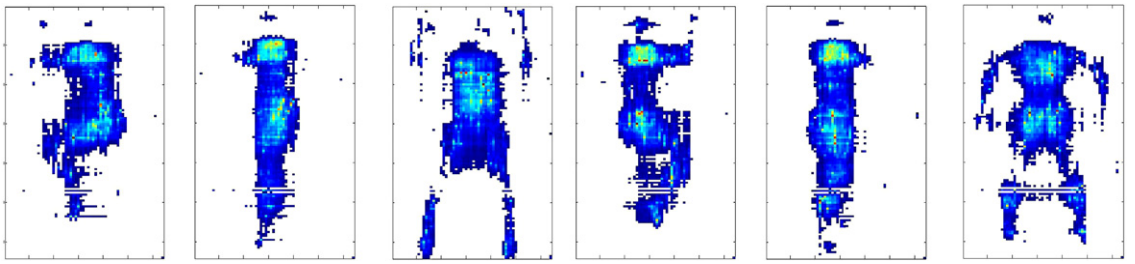

Fig. 1. Human body pressure image samples.

specifically, one of the main problems for post-surgical patients and elderly patients is formation of pressure ulcers [8]. Pressure ulcers, or bedsores, are localized injury to body tissue, usually near the bone, resulting from low blood circulation and lack of movement. Pressure ulcers are a serious, life-threatening disease, they develop quickly and are expensive to treat once they have progressed far enough [9]. Prevention is the best way to combat this problem, and in many cases, pressure ulcers are preventable. Hospital staff need to be attentive to patients that are more susceptible to this condition, and take action to relieve pressure on the highly sensitive locations by changing their sleep postures. Current best practices in nursing involve moving patients every several hours. However, there is no guarantee that patients remain in one posture in the meantime, or even if patients are turned onto already sensitive locations.

Given these applications, autonomously monitoring patients during recovery is desired, especially when pressure ulcers can develop very quickly. The goal of any medical system that prevents the formation of pressure ulcers requires the analysis of sleeping postures, as well as notifications of susceptible and impending pressure points on the patient's body. Therefore, there is a need for automatic sleep posture monitoring.

To date, researchers have proposed different ways to monitor sleep posture automatically. Video cameras and microphones have been used previously to study sleep posture patterns. For example, Nakajima et al. [10] prototyped a system based on visual signals to analyze sleep posture changes. However, lighting issues are a main drawback of using video. Low light levels at night add noise to the images, and even when near-infrared cameras are used [11] the images still produced non-uniformity and artifacts. Furthermore, video and voice recording raise serious privacy concerns for users.

Inertial sensors, including accelerometers, gyroscopes and magnetometers, are another applied technique used to monitor sleep. Sadeh and Acebo attached several tri-axial accelerometers on people's limb to monitor sleep patterns via an actigraph [12]. Kishimoto et al. deployed 14 wearable motion sensors on users at home for remote sleep posture analysis [13]. The main downside to this technique is that sensors have to be attached to the body which can be uncomfortable or burdensome to the users. Recent work with ECG measurements has shown that the morphology of the human QRS complex can be used to estimate body posture [14].

Alternatively, dispersed pressure sensors embedded in the mattress can record when changes in body posture occur. This method is unobtrusive and does not interfere in the comfort of users. Also it is a stable medium that is not affected by changes in the environment. Hoque et al. facilitated a mattress with wireless-powered accelerometers to record movement activity [15]. Jones et al. developed a bedsheet system with 24 pressure sensors [16]. However, such prior work focused on detecting posture change rather than recognizing body posture. Similarly, Foubert et al. were able to detect changes from lying to sitting posture [17]. Mattress indentation is another modality to assess sleeping patterns [18].

In this paper, we focus on sleep posture analysis using pressure sensors. We employ a dense pressure sensitive textile bedsheet and apply pressure image analysis for sleep posture recognition. Our contribution in this work is threefold. First, we propose a framework for automatic sleep posture analysis based on a dense pressure sensitive bedsheet prototype (64×128 sensors) designed using e-textile material. We would like to argue that pressure image analysis is more challenging than video image analysis due to incomplete body pressure maps and self occlusions. Second, we define and discuss a set of geometric features from pressure images for posture analysis. These features are effective not only in distinguishing different postures but also in characterizing each posture with physical meanings (the details about geometric features will be elaborated in Section 3). Third, we develop *three* heuristics based on sparse representation to classify sleep postures. We evaluate our proposed methods with 14 subjects for 6 common sleep postures (see Fig. 1) in static evaluation trials, and 8 h continuous monitoring trials where we use transitional information from one posture to the next. The proposed method exhibits better performance in terms of accuracy and robustness than traditional classification methods.

In contrast to previous work which has generally focused on recognizing three postures, Left Fetus, Right Fetus, and Supine postures [19,20], we describe here a classification system that includes additional harder and commonly used postures. These being Left Log, Right Log, and Prone. The log postures are positions where subjects are lying on their sides with legs almost straight. In many hospital settings, these postures are supported with pillows behind their shoulders and back. The aim of such postures is to ameliorate the possibility of developing pressure ulcers on the hips, shoulders, and buttocks.

The remaining part of the paper is organized as follows. Section 2 describes the overall design of this monitoring system which incorporates a pressure sensitive bedsheet. Section 3 describes the algorithmic process of sleep posture recognition by extracting pressure image features and classification using the theory of Sparse Representation. Experimental setup and results are provided in Section 4. Finally, future work and a conclusion are discussed in Section 5.

Fig. 2. Pressure sensitive bedsheet.

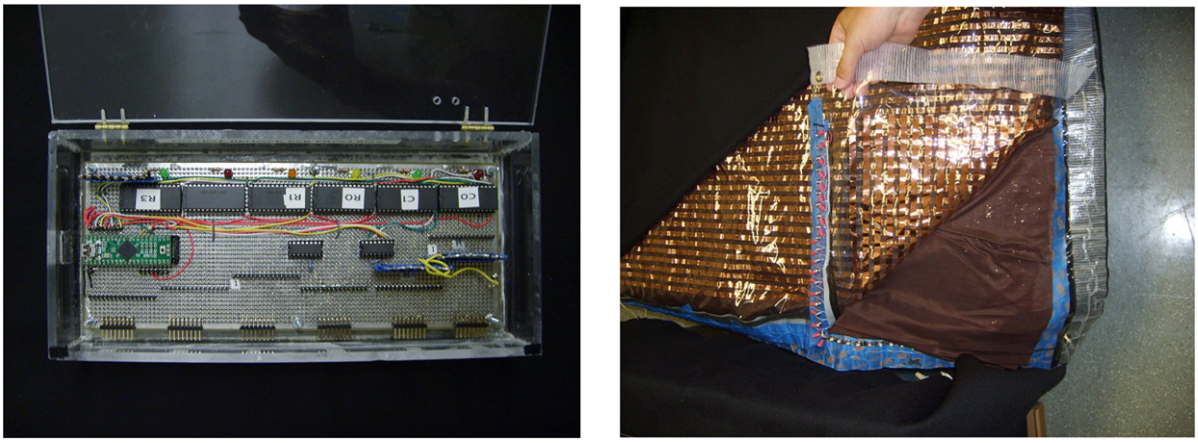

(a) Scanning module. (b) E-textile between conductive lines.

Fig. 3. System components.

2. Bedsheet design

In this section, we present the design of the bedsheet system. The goal of this specialized bedsheet is to record the pressure distribution of the body while sleeping and then perform data analysis for medical applications. For instance, when a patient has had recent surgery around the left hip, limited pressure should be applied on that area and a left-lying posture should not be allowed. When the bedsheet system detects that the patient is lying on his left side for a period of time, the patient or caregivers can receive an alert to change the posture. Accordingly, the bedsheet system is designed with the following consideration:

- High-resolution: The bedsheet should offer high resolution for pressure sensing. Given enough resolution, it is possible to quantify the applied pressure on body parts and enable high accuracy medical diagnosis.
- Comfort: The user should feel comfortable lying on the sheet. Also, it should be easy to deploy in the home or hospital.
- Low-cost: For widespread use, the cost for the bedsheet implementation should be low and affordable for most people.

There are some existing sensor products [21,22] that comprise many piezo-electrical pressure sensors. However, none of them meet the above design criterions for widespread applications.

Figs. 2 and 3 show the prototype of our bedsheet system. The system consists of three components: a 64×128 pressure sensor array, a data sampling unit, and a tablet for data analysis and storage. The sensor array is based on eTextile material which is a fiber-based yarn coated with piezo-electric polymer [23]. The initial resistance between the top and bottom surfaces is high. When extra force is applied on the surface of the eTextile, the inner fibers will be squeezed together and the electrical resistance will become smaller.

(a) One subject on the bedsheet system. (b) Pressure image.

Fig. 4. System demonstration with one subject sleeping in a right fetus posture.

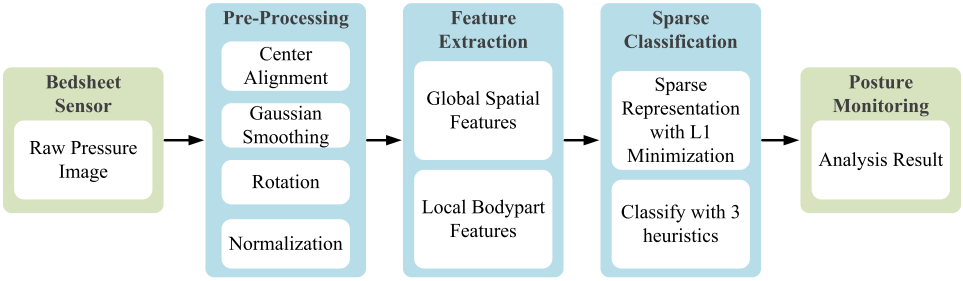

Fig. 5. Sleep posture recognition framework.

The textile sensor array has a three-layer sandwiched structure: the top layer is normal fabric uniformly coated with 64 parallel conductive lines; an eTextile layer in the middle; and a bottom layer with 128 conductive lines (perpendicular to the top 64 lines). Within this structure, each intersection of conductive lines becomes a pressure sensitive resistor. In total there are effectively 8192 pressure sensors.

When an electrical potential is applied between one of the vertical and horizontal conductors, the resistance at the intersection point can be measured. By scanning all of the vertical and horizontal lines in sequence, a resistance map can be created of the entire bedsheet and, after converting to digital 8 bit values, a pressure image results.

Fig. 4(a) shows an example of a user lying on the bedsheet. The subject sleeps on the bedsheet in a right fetus posture, and the corresponding pressure image is illustrated in Fig. 4(b). We can see that body parts (such as hip, legs) are shown clearly in the pressure image due to the dense sensors in the bedsheet. It is helpful to characterize the geometrical features of sleep postures and posture classification, which will be discussed in detail in the next section.

3. Framework for sleep posture analysis

Fig. 5 shows the sleep posture analysis process. The central three steps, Pre-processing, Feature Extraction, and Sparse Classification will be discussed in this section.

3.1. Pre-processing

The pre-processing on the raw pressure images is required so that the images can be standardized in such a way as to enable successful classification. The raw images contain noise and artifacts that affect classification, and pre-processing mitigates these side effects as much as possible.

- The subject can be located anywhere on the bedsheet, so to correct this, the images are aligned to a common center of mass and relocated to the center of the image.
- A smoothing filter of a symmetric 5×5 unit normal distribution is applied. This smoothing minimizes the effect of noise in the pressure map.

Table 1
Global spatial features.

No.	Name	Description
1	Coverage	Proportion of image covered
2	Per25	Coverage of 25% of pressure
3	Per50	Coverage of 50% of pressure
4	Per75	Coverage of 75% of pressure
5–12	Reg1–Reg8	Coverage over 8 fixed rectangular regions
13	Symmetry	Measure of pressure symmetry
14	Balance	Measure of pressure on both sides of image
15	DirCurve	Measure of curvature of pressure image

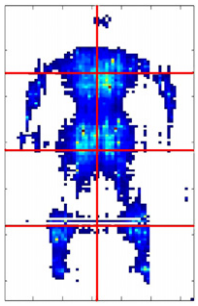

Fig. 6. Coverage by regions: features 5–12.

- The images are rotated so that the dominant axis of the body shape is aligned vertically in the image. The dominant axis is found by an eigenvector calculation by approximating the human body geometry as an ellipse. This accounts for the different lying angles for the subjects.
- The images are normalized so that the sum of pixel weights is one. This step attempts to counteract the effects of different body masses of patients.

3.2. Feature extraction

Traditional feature extraction methods on images include dimension reduction techniques. Widely popular is Principal Component Analysis [24] which relies on finding the dominant orthogonal axes which maximizes the statistical variances in the data. PCA is largely data dependent and is a general method to find macro structure in datasets. This method has been applied to sleep posture recognition in current literature [25].

In this work, we propose a different method of feature extraction for posture classification that is based on the geometry of the pressure images. It is more attuned to the physical characteristics of the body shape and has a definite physical meaning. An advantage of using these proposed features over PCA reduction is the processing time required to extract these features; our proposed features are based on simple geometry.

In all, we propose 32 features to be extracted from each of the pressure images. The features are described as either Spatial features or Body part features. Spatial features are those features that describe global aspects of the image such as the proportion of the image that is covered by the subject, the symmetry of the image, and direction of any curvature in the pressure image. Body part features are localized features that describe the location and size of expected body parts such as the hip and shoulder.

Refer to Table 1 for a full a listing of the global Spatial features and Table 2 for the localized Body part features. A more detailed explanation of the features follows here. Unless otherwise stated, we will assume the x axis is along the short side of the bedsheet, the y axis runs along the long side of the bedsheet.

Coverage features (1–12). The first feature is Coverage which is the number of pixels that have non-negative sensor values divided by the total number of pixels. The next 3 features only consider coverage for the pixels that contain 25%, 50%, 75% of the total pressure. Features 5–12 relate to coverage by regions. The regions are 8 equally sized subdivisions of the image (see Fig. 6). Given that the original dimensions of the image are 64×128 pixels, the region sizes are 32×32 pixels.

Symmetry and balance (13, 14). Symmetry is the sum of the absolute value of the difference of pixels on either side of the center image line. A supine posture would have more symmetry than a side posture. Balance is the sum of the difference of pixels on either side of the center image line. This is different to the Symmetry measure in that we do not take the absolute value of the difference of pixels. The resulting measure describes which side of the image contains most of the pressure.

Direction of curvature (15). This measure detects the dominant direction of curvature of the body image. A person lying on one side will have a detected body curvature, whereas a supine position should exhibit a straighter pressure image. The steps to extract this feature metric are as follows:

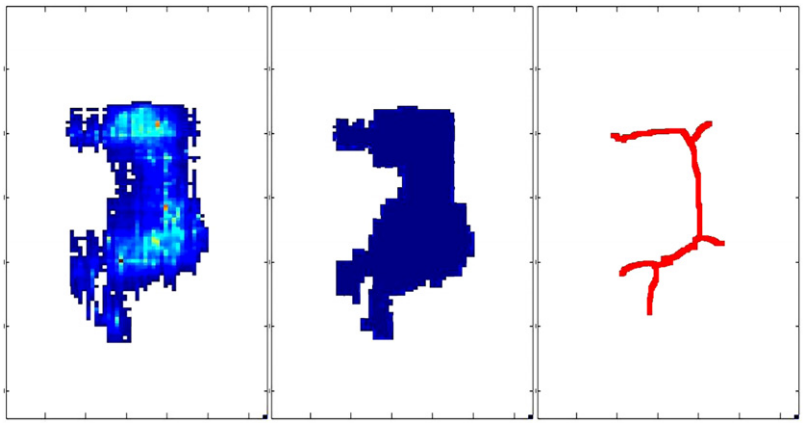

Fig. 7. Direction of curvature feature: Left: original image. Middle: thresholded image. Right: skeletonized image.

Table 2
Local geometrical body part features.

No.	Name	Description
16, 17	HipPoint	(x, y) location of hip location
18–21	HipBox	$(x, y$, width, height) of bounding box of hip
22	HipArea	Area in pixels of bounding box of hip
23	HipPtoBox	Ratio of hip location to bounding box width
24, 25	ShPoint	(x, y) location of shoulder location
26–29	ShBox	$(x, y$, width, height) of bounding box of shoulder
30	ShArea	Area in pixels of bounding box of shoulder
31	ShPtoBox	Ratio of shoulder location to box width
32	HipShDist	Hip to shoulder distance

- Create a binary image that contain pixels that are above a suitable threshold. The choice of threshold is obtained experimentally, although a reasonable estimate is 50% of the peak sensor value.
- Skeletonize the binary image by finding midpoints of boundary pixels (see Fig. 7).
- Remove joint pixels from the skeleton so that each curve is separated. Remove curves that are shorter than 5 pixels.
- For all pixels along the curve, find the angle bisector. The director of curvature is taken as the sum of the y components of the angle bisectors, i.e. in the lateral axis of the bedsheet.

Hip features (16–23). Since pre-processing of the image is done initially, we make the assumption that the hip is located in the quarter of the image below the center of mass of the pressure image. An estimate of the hip location is taken to be the pixel that is located at the weighted center of pixels in this quarter image. The bounding box around the hip is the rectangular region of the pixels that contain 75% of the pressure value within the quarter image below the center of mass of the pressure image. The ratio of hip location to bounding box width provides a measure that shows where the hip location is in relation to the bounding box of the hip.

Shoulder features (24–31). Similar to the hip features (16–23) above, we extract the same information for the shoulder. A similar assumption applies to the quarter image above the center of mass for the shoulder location. Fig. 8 shows a sample of the locations and bounding boxes of the hip and shoulders. Finally, Feature 32 is the pixel distance between hip and shoulder locations.

Since all the features described above are on different scales, the feature values are scaled and shifted so that the resulting values are in the range $[0, +1]$.

3.3. Classification preliminaries

Before we investigate Sparse Classifiers, we review the progression of classification basics from Nearest Neighbor to Nearest Subspace, then to Sparse Classification.

The Nearest Neighbor classifier simply finds the closest training sample in the feature space to provide a prediction for a test sample. Euclidean distance is the most common measure of closeness between the test sample and the training samples given that the feature space consists of continuous variables.

With a training dataset of n samples, and each training sample having m dimensions (features), let each sample be $a_i \in \mathbb{R}^m$. Now given a new test sample $y \in \mathbb{R}^m$, the nearest neighbor is the training sample that minimizes the distance to the test sample:

$$\arg\min_i \|y - a_i x\|_2, \tag{1}$$

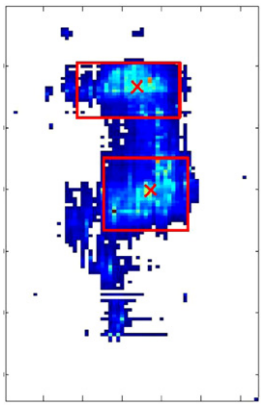

Fig. 8. Hip and shoulder features.

where x is an identity vector and we assume that all features have been scaled to a common range. The prediction is the class to which the nearest sample belongs.

The nearest neighbor classifier is a popular classifier because of its simplicity and robustness to noise as long as there is sufficient training data. However it has several disadvantages such as high dimensional data reducing the effectiveness of classification. Some features (dimensions) may be more important than others in classification and Nearest Neighbor does not take this into account.

The Nearest Subspace classifier [26] extends Nearest Neighbor to include information about assigned class labels. Instead of finding the closest training sample, Nearest Subspace finds the closest subspace that is spanned by training samples belonging to that class. So given a training dataset of n samples, and each training sample having m dimensions (features) and having a class label k, let the training samples for class k be A^k. The training samples are column vectors placed side by side. Now given a new test sample $y \in \mathbb{R}^m$, the nearest subspace is the class that minimizes the distance of y to the subspace spanned by all the training samples of that class:

$$\arg\min_k \|y - A^k x\|_2, \tag{2}$$

where x is a vector of weight coefficients. For each class k, the test sample y can be represented by a weighted combination of the training samples in class k if we consider each of the training samples as basis vectors in the subspace spanned by the training samples. So for each class k, $A^k x$ represents a reconstructed sample similar to y. This classifier assigns the class label which minimizes the reconstruction error. The solution to Nearest Subspace can be found using convex optimization with the constraint that all weights are non-negative. Without this constraint, the solution degenerates in this overdetermined system.

The Nearest Subspace classifier finds a representation of a test sample in the subspaces spanned by class training samples. We extend this idea further using Sparse Representation. The general idea is to represent the test sample using all the training samples, initially without regard to the classes of the training samples. By imposing sparsity constraints on the representation of the sample, a different type of classifier can result. The following section describes classification using Sparse Representation of samples.

3.4. Classification using sparse representation

Sparse Classification has been used previously in other medical analysis and has been shown to have effective performance over a wide range of applications [27]. The classification method comes from the theory of Compressed Sensing [28] which proposes that data exhibits sparsity in some transformed representations. That is, a signal can be represented as a sparse signal in a transformed feature space, and can be accurately reconstructed with a lower sampling rate than the Nyquist–Shannon rate.

Given a dataset of n samples, with each sample having m dimensions (features), define the data matrix $A \in \mathbb{R}^{m \times n}$ that comprises these m-element column vectors arranged side by side. Now given a new sample $y \in \mathbb{R}^m$, can a solution $x \in \mathbb{R}^n$ be found such that x is described in terms of the dataset? i.e. can we find x that satisfies

$$y = Ax. \tag{3}$$

So y is a linear combination of the columns in the data set, and $x = [x_1, x_2, \ldots, x_n]^T$ is an unknown vector of coefficients. This linear system is underdetermined when there are more unknowns than equations, and hence there are infinitely many solutions for x. This is the case for our formulation of posture classification in this paper. However, if certain constraints are imposed, then a unique solution for x exists and will accurately represent the original sample. There are 3 main sparsity constraints on x that have been considered in literature.

- l_0 sparsity is defined to minimize the number of non-zero elements of x. Solving for x has been shown to be NP-hard [29].
- l_2 sparsity is the efficient least squares solution, however this is not always equivalent to the l_0 solution.
- l_1 sparsity is defined as the minimal sum of absolute values of elements of x. Candes et al. [28] have proved that l_1 sparsity is equivalent to l_0 and, moreover, can be solved as a convex optimization problem:

$$\hat{x} = \arg\min_x \|x\|_1, \quad \text{s.t. } y = Ax. \tag{4}$$

The sparse representation of a sample is used in classification by matching this representation to a set of class labels. The dataset A comprises training samples and each sample has been assigned a class label, C_n. Let each training sample be represented as a column vector, a_{ij}, where j is the sample number within class i. The number of samples need not be the same for each class. The data matrix A is shown here with samples grouped together in their classes:

$$A = \Big[\underbrace{\begin{matrix} | & | \\ a_{11} & a_{12} \\ | & | \end{matrix}}_{\text{class 1}} \cdots \underbrace{\begin{matrix} | & | \\ a_{21} & a_{22} \\ | & | \end{matrix}}_{\text{class 2}} \cdots \underbrace{\begin{matrix} | & | & \\ a_{k1} & a_{k2} & \cdots \\ | & | & \end{matrix}}_{\text{class } k} \Big]. \tag{5}$$

Any test sample y is represented by a linear combination of the training samples:

$$y = a_{11}x_1 + a_{12}x_2 + \cdots + a_{kj}x_n, \tag{6}$$

where k is the number of class labels and j is the number of training samples for the k-th class.

The l_0 minimized sparse solution for x will have only a small number of non-zero elements. The training samples that correspond to the non-zero elements are those that can represent the new sample well. We propose 3 heuristics to select the class label given a sparse solution for x and the dataset with training labels as follows.

- Maximum Coefficient (MC). The class label belonging to the training sample that corresponds to the largest coefficient of the sparse solution of x is the predicted class label:

$$\hat{k} = C_{\arg\max_i(x_i)}. \tag{7}$$

- Maximum Sum of Class Coefficients (MSCC). The predicted class label is the class whose sum of coefficients of x is maximized:

$$\hat{k} = \arg\max_k \left(\sum_{i \in a_{ki}} x_i \right). \tag{8}$$

  In other words, for each class k, take the sum of the coefficients of x that correspond to the training samples belonging to that class. The predicted label is the class that maximizes these sums. The training samples that are most closely represented to the test sample should correspond to the bulk of elements of the sparse solution to x.
- Minimum Class Residual (MCR). An alternate choice for a heuristic to predict the class label is to find the class that minimizes the class residual. The residual is the error between the test sample and the reconstructed sample based on the sparse solution to x:

$$residual = \|y - A\hat{x}\|_2. \tag{9}$$

  So the predicted class is

$$\hat{k} = \arg\min_k \|y - A_{ki}x_i\|_2. \tag{10}$$

Each of these 3 heuristics are evaluated in Section 4.

3.5. Hidden Markov model for continuous posture evaluation

In our experiments on the continuous sleep posture monitoring, we investigate the use of Hidden Markov Models [30,31] on time sequential images. The Hidden Markov Model (HMM) is a stochastic process where internal states of a system depend only on previous states and are hidden from direct observation. In our application, the hidden states are the sleep postures of the subjects and the direct observations are the pressure images from the bedsheet. Using HMMs, the sequence of postures is ascertained from the sequence of pressure images and knowledge of the state transition and observation probabilities.

The formulation of HMM is as follows (refer also to Fig. 9). We represent N postures as N hidden states, $\{S_1, S_2, \ldots, S_N\}$. Postures can change to another posture according to an assigned transition probability a_{ij}:

$$a_{ij} = \Pr(s_{t+1} = S_j \mid s_t = S_i), \tag{11}$$

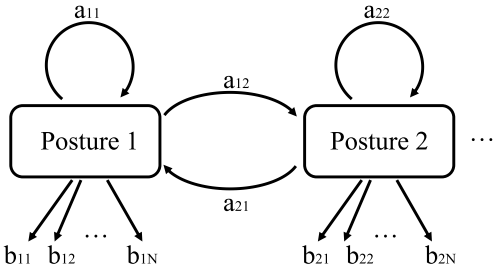

Fig. 9. Hidden Markov model with hidden postures. Only 2 postures are shown in this diagram.

where s_t is the posture at time t. So a_{ij} is the probability that a subject who is currently sleeping in posture i changes to posture j. Sleeping postures can remain in one state for an indeterminate amount of time, i.e. the current state can transition to the same state, and this allows time scale invariance in this model. With N postures, there are $N \times N$ transition probabilities. In our experiments in Section 4, the state transition probabilities for each subject are calculated from the training data.

Although the direct observable outputs from our system are the pressure images, we apply our classification method on each image to produce predictions for postures. So for each state S_i, there is the probability b_{iq} that posture q is predicted. Let v_q be the predicted posture, then the observation probability, b_{iq}, is the probability of predicting posture v_q given the hidden posture is S_i:

$$b_{iq} = \Pr(v_q \mid s_t = S_i). \tag{12}$$

So, for every observed pressure image at time t, the HMM calculates all the observation probabilities for the N predicted postures. The actual probability calculation is based on a confidence measure from each of our heuristics of the Sparse Classifier.

Our proposed confidence measure is a relationship between first best match and second best match from a different posture [32]. For example, the Maximum Coefficient (MC) heuristic finds the posture that corresponds to the training sample with the largest coefficient of the sparse solution. Let the maximum coefficient for this predicted posture v_q be m_1. Let the second best coefficient of the sparse solution that does not have the same predicted posture v_q be m_2. Then we can calculate the observation probability as:

$$\frac{m_1}{m_1 + m_2}. \tag{13}$$

Since the solution of the coefficients is sparse, most of the observation probabilities are zero. The observation probability for the Maximum Sum of Class Coefficients (MSCC) heuristic is similar where the first best match m_1 is the maximum sum of the class coefficients and the second best match m_2 is the next best sum of the class coefficients of a different class. The Minimum Class Residual (MCR) is adjusted to account for the minimization:

$$1 - \frac{m_1}{m_1 + m_2}, \tag{14}$$

where m_1 is the minimum class residual and m_2 is the residual for the next best class. We present the HMM results for the confidence measures for our 3 heuristics in Section 4.3.

4. Experimental results

4.1. Experimental setup

We ran two sets of studies in the lab to evaluate the performance of the system for sleep posture monitoring. The first study was designed to collect training data and to evaluate short term performance over fixed intervals. The second study analyzed the performance of the system for overnight continuous monitoring. The results of the second study are given in Section 4.3.

This section describes the performance of the first study. There are 14 subjects in the experiment, where 9 subjects are male and 5 subjects are female. The weight of the subjects ranges from 55 to 85 kg, and height between 155 and 185 cm, as shown in Table 3. The bedsheet system was deployed on a standard twin-size coil spring mattress during the experiments (see Fig. 2).

In Idzikowski's study of 1000 people [33], left and right fetus postures, i.e. with legs bent, are most common at 41%. The other side lying postures, i.e. with straight legs, account for 28% of positions. We refer to these as log postures. Supine (8%) and prone (7%) postures are the next most common. Therefore, for the experimental evaluation, we investigate the 6 postures including Left-Log (LL), Left-Fetus (LF), Right-Log (RL), Right-Fetus (RF), Prone (P) and Supine (S). The examples of these postures are shown in Fig. 10.

Table 3
Training subjects.

	Gender	Age	Weight (kg)	Height (cm)
1	Female	25	57	158
2	Female	31	53	162
3	Female	27	65	168
4	Female	24	58	162
5	Female	23	60	165
6	Male	27	70	178
7	Male	26	74	172
8	Male	22	62	170
9	Male	35	70	180
10	Male	39	66	178
11	Male	28	72	184
12	Male	27	68	175
13	Male	29	63	173
14	Male	26	65	176

Table 4
Accuracy comparison to other classifiers.

	Precision	Recall	f-measure[a]
C4.5 Decision Tree	57.0%	56.8%	56.9%
k-Nearest Neighbor	64.7%	62.1%	63.4%
Nearest Subspace	77.0%	76.5%	76.8%
Sparse Classifier (MC)	**65.4%**	**61.0%**	**63.1%**
Sparse Classifier (MSCC)	**83.1%**	**82.7%**	**82.9%**
Sparse Classifier (MCR)	**83.5%**	**82.9%**	**83.2%**

[a] f-measure is the harmonic mean of precision and recall.

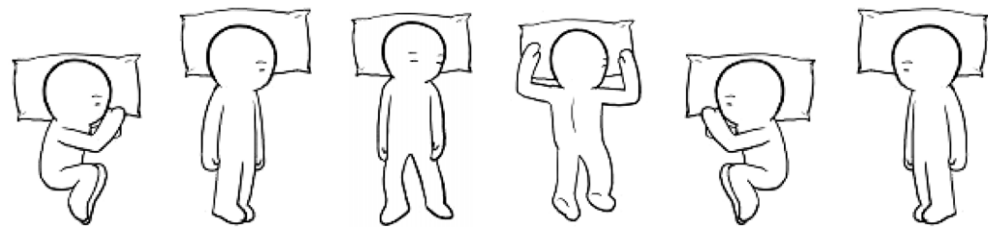

(a) Right Fetus. (b) Right Log. (c) Supine. (d) Prone. (e) Left Fetus. (f) Left Log.

Fig. 10. Six postures used in experiments.

In the data collection, 40 samples were recorded for each of the 6 postures for each subject. At fixed intervals, the pressure image of the subject's posture was recorded while the subject maintained a comfortable sleeping position. Variations in body, arm and leg positions were allowed and the system is tested on a range of positions that fall within the 6 defined postures. All postures include a standard queen size pillow for the head. Testing was carried out with Leave One Out Cross Validation by subject, i.e. test on one subject's data with the training data from all the other subjects. Repeat this for each subject. Sparse classifiers are implemented using the CVX convex optimization package [34].

The time to process each image using this method is 0.21 s on a single core 3.0 GHz processor, of which 0.012 s is used to extract the geometric features. Given that posture does not change much while sleeping, this timing is sufficient for this application and can be implemented within an embedded microprocessor.

The following experiments were tested against ground truth labeling. Fig. 11 shows a video camera rigging for the ground truth visual image collection. All posture labels were marked manually from the visual images.

4.2. Sparse classification results

Table 4 summarizes the precision and recall results of 6 posture classification using the set of geometric features with different classifiers. The Sparse Classifiers with Maximum Sum of Class Coefficients (MSCC) heuristic and Minimum Class Residual (MCR) heuristics show a 20% improvement in accuracy over Decision Tree and Nearest Neighbor classifiers, and 6% improvement in accuracy over Nearest Subspace.

We note that the Maximum Coefficient (MC) heuristic does not show any improvement in the accuracy over Nearest Neighbor. The reason was given previously and is such that after the transformation into the sparse domain, the Maximum Coefficient (MC) is a metric similar in nature to Nearest Neighbor. It essentially finds the single training sample that maximizes its representativeness to the test sample, and does not take into account the class membership. Nearest Subspace

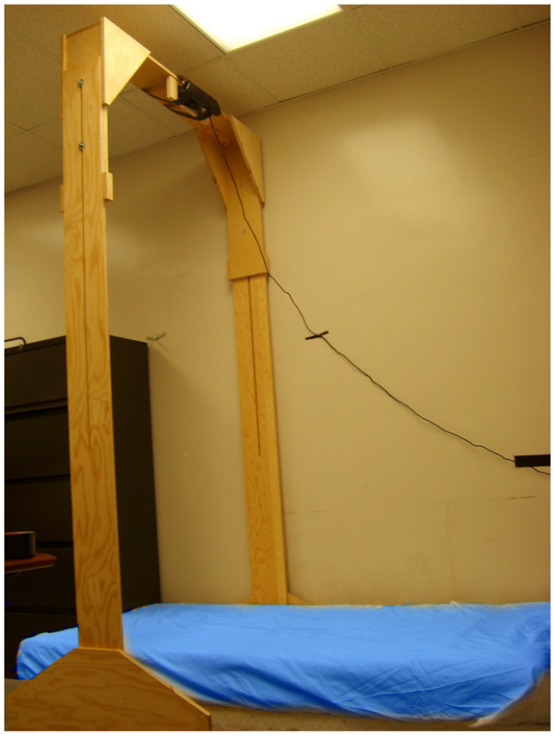

(a) Camera frame for overhead recording.

(b) Sample of overhead image.

Fig. 11. Video recording setup for ground truth labeling.

Table 5
Confusion matrix nearest neighbor.

	LL	LF	P	RL	RF	S	Recall
LL	123	6	7	26	41	83	43%
LF	3	194	14	39	3	33	68%
P	1	27	234	0	19	5	82%
RL	46	21	0	171	6	42	60%
RF	45	9	14	25	185	12	64%
S	42	6	3	20	5	210	73%
Precision	47%	74%	86%	61%	71%	55%	

Table 6
Confusion matrix nearest subspace.

	LL	LF	P	RL	RF	S	Recall
LL	143	0	2	51	41	20	66%
LF	3	243	21	30	4	6	79%
P	10	16	253	0	20	4	83%
RL	27	17	0	183	2	9	76%
RF	44	7	10	13	262	5	77%
S	59	3	0	9	1	242	77%
Precision	50%	85%	88%	62%	90%	84%	

does take into account class membership and hence exhibits a fair accuracy. The downside to Nearest Subspace is that it requires multiple optimization problems to be solved, i.e. one for each class. We note that the Sparse Classifiers only require a single run since it treats all the class samples as one sample space.

We look more closely at the results of the Spare Classifiers and note the confusion matrices given in Tables 5–9. Table 5 shows the confusion matrix for Nearest Neighbor classifier and we note the similarity with the Maximum Coefficient Sparse Classifier (MC) in Table 7.

Generally, the log postures are harder to recognize than the other postures. Recall for both Left Log and Right Log are always lower than the other 4 postures, while the precision rates are generally lower but not always. The log postures are

Table 7
Confusion matrix sparse classifier (MC).

	LL	LF	P	RL	RF	S	Recall
LL	149	29	24	19	23	42	52%
LF	15	168	26	30	18	29	59%
P	9	24	202	6	20	25	71%
RL	40	25	5	176	22	18	61%
RF	11	22	23	19	194	21	67%
S	44	13	11	9	11	198	69%
Precision	56%	60%	69%	68%	67%	59%	

Table 8
Confusion matrix sparse classifier (MSCC).

	LL	LF	P	RL	RF	S	Recall
LL	207	6	2	15	6	50	72%
LF	4	249	14	6	9	4	87%
P	1	22	245	1	12	5	86%
RL	14	27	1	219	12	13	77%
RF	0	9	14	3	262	2	90%
S	30	6	2	1	3	244	85%
Precision	81%	78%	88%	89%	86%	77%	

Table 9
Confusion matrix sparse classifier (MCR).

	LL	LF	P	RL	RF	S	Recall
LL	202	8	5	18	5	48	71%
LF	2	252	18	5	6	3	88%
P	1	22	249	1	10	3	87%
RL	12	28	2	225	10	9	79%
RF	0	11	15	5	257	2	89%
S	27	9	3	1	3	243	85%
Precision	82%	76%	85%	88%	88%	79%	

most similar to each other since both have legs outstretched and arm positions can vary. The next most similar posture is Supine. This is seen in all of the confusion matrices as high counts for predicted switched Left Log and Right Log, and Supine.

Fig. 12 shows two examples of misclassifications of hard log postures. The left image shows Left Log posture that is incorrectly identified as Right Log. This typical kind of error can be explained from the pressure map that is extended behind the subject's back. Hence misclassifications can occur since the pressure image now looks like a Right Log image. Similarly, the right image shows Right Log posture that is incorrectly identified this time as Supine. Visually, this image is hard to not identify as Supine.

4.3. Overnight continuous monitoring

To further evaluate the accuracy of the pressure sensitive bedsheet system, we tested the posture analysis for continuous overnight monitoring. In this study, we monitored 3 patients over 3 nights on the bedsheet. Overhead video images of the subjects were recorded to manually extract the ground truth postures. Roughly 2600 pressure images were recorded for each overnight session lasting 7–9 h. Since subjects do not move much while sleeping, the sampling rate was decreased to 10 s per sample for the sake of memory constraints on the tablet.

We analyzed the results using the HMM framework with subject dependent testing. With three complete overnight data for each subject, we used two of the sets for subject training and tested on the third, and repeated with cross validation. The results shown in Table 10 compare two classification schemes: one with Hidden Markov Models and the other with plurality voting over sliding window of size 10. Both of these classification methods showed small improvements in the accuracy of posture analysis over long durations and sequential pressure imaging, compared to static posture analysis in the previous sections.

For sliding window plurality voting, the predicted posture is chosen as the posture with the relative majority compared to the other postures, and is updated with a sliding window of fixed size over the set of consecutive previous images. In each group of consecutive samples, the simple plurality vote of the predicted test sample classifications is taken as the classification for that grouping of image samples, i.e. the posture that is predicted most frequently.

Overall, the results of continuous monitoring study show that classification accuracy can be improved when sequential static images are available. The HMM based sequential methods show roughly a 2%–3% improvement over static image classification for the Maximum Sum of Class Coefficients (MSCC) and Minimum Class Residual (MCR) heuristics.

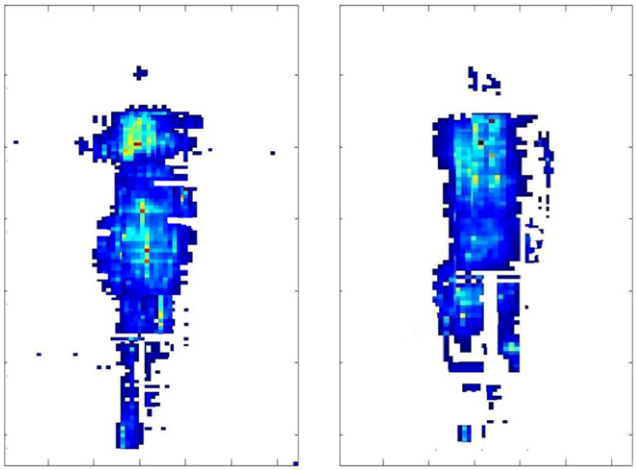

(a) Left Log posture misclassified as Right Log.

(b) Right Log posture misclassified as Supine.

Fig. 12. Misclassified postures.

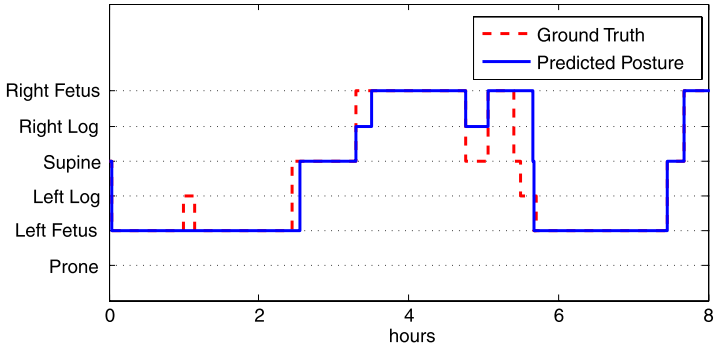

Fig. 13. An example of one subject's 8 h continuous monitoring study.

Table 10
Experimental results for overnight studies.

	Precision	Recall	f-measure
HMM with MC	78.4%	73.6%	75.9%
HMM with MSCC	86.5%	84.7%	85.6%
HMM with MCR	86.0%	84.4%	85.2%
Sliding window plurality with MC	73.9%	76.5%	75.2%
Sliding window plurality with MSCC	83.7%	84.5%	84.1%
Sliding window plurality with MCR	83.8%	84.8%	84.3%

Interestingly, the HMM with Maximum Coefficient method shows the largest improvement. This may be explained by the fact that Nearest Neighbor type methods benefit most by the clustering of points as more data is considered. A sliding window size of 10 improves the classification by a percentage point over static image classification, however this may not be statistically significant over a small total sample size.

Fig. 13 shows the result of one of the test subjects for an 8 h overnight continuous monitoring session with predicted and true postures given. The subject is a typical sample of the progression of posture sequences. Here the subject had 12 discernible posture changes.

4.4. Stability analysis

In this section, we analyze the robustness of the classification by firstly investigating the variation during cross validation. We also investigate whether patient height affects classification results. Stability is a measure that describes how closely the classifier evaluates results if given different data. Fig. 14 shows the classification variation for the 6 postures for each of the classifiers.

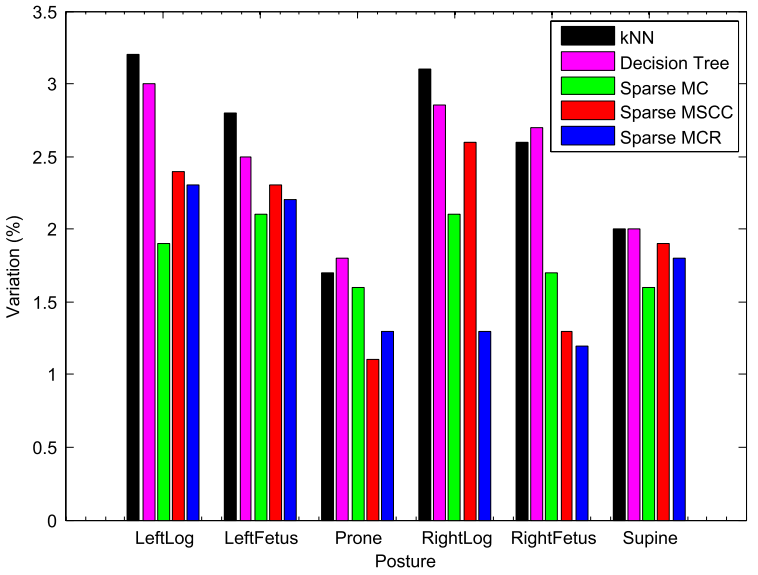

Fig. 14. Classification variation for 6 postures.

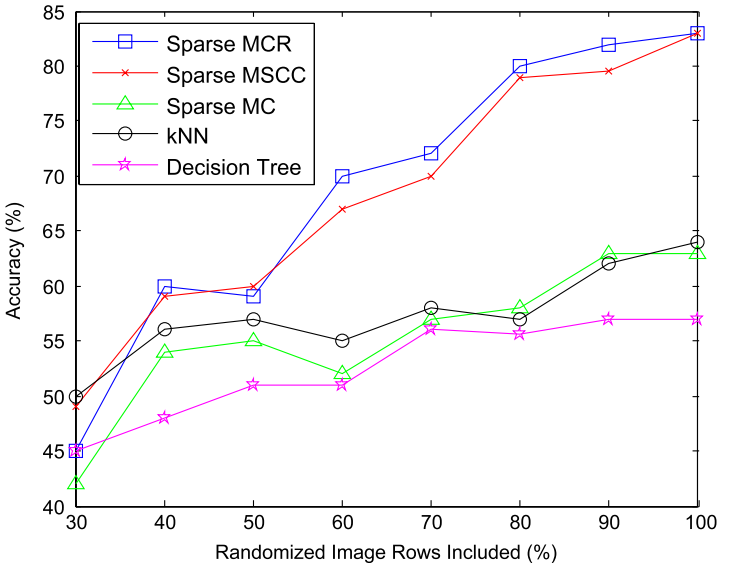

Fig. 15. Classification robustness with random row deletions.

The Sparse Classifiers have smaller variation values than the other traditional classifiers. This indicates that sparse classification is a more stable classification method. The log postures have a higher variation in classification accuracy than the other postures. This is explained by the higher variation in weight distribution for these postures. In our data, the log postures vary greatly between fully lying on the side and lying on the back.

Although the Maximum Coefficient (MC) Sparse Classifier achieves the same accuracy as Nearest Neighbor, it does perform better when considering its enhanced stability.

We also consider the robustness of the algorithm with regards to input errors, such as from disconnected wires in the bedsheet. The effect of this would be missing rows or columns of data in the pressure image. Fig. 15 shows experimentally how a random number of failures of bus lines will affect the accuracy of the classification result. Roughly 20% of the hardware connections can fail with only a 4% drop in classification accuracy.

Table 11 shows results for a subset of patients based on subject height. The tested groups were subjects with height below 165 cm (approximately 1/3 of the total patients), subjects with height above 178 cm (approximately 1/3 of the total patients), and the remaining subjects. It is interesting to note that, using our Sparse Classifier, the taller subset of patients did exhibit a higher classification accuracy compared to the mean accuracy, while the shorter subjects showed a lower classification accuracy. This is not true for the Nearest Neighbor classifier. The fact that the Nearest Neighbor classifier does

Table 11
Accuracy (f-measure) of subjects grouped by height.

	Subjects $\leq$ 165 cm	165 cm $<$ Subjects $<$ 178 cm	Subjects $\geq$ 178 cm
k-Nearest Neighbor	61.1%	67.3%	60.0%
Nearest Subspace	75.5%	77.1%	76.0%
Sparse Classifier (MC)	61.1%	66.1%	62.1%
Sparse Classifier (MSCC)	80.6%	83.0%	85.6%
Sparse Classifier (MCR)	81.1%	83.1%	85.4%

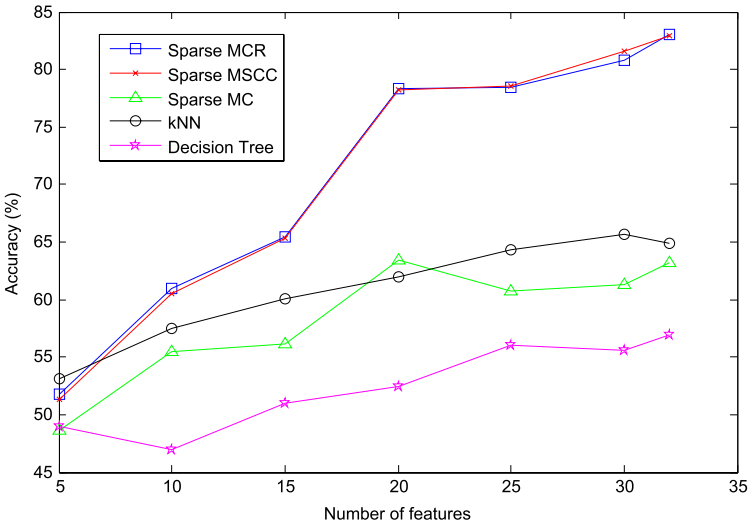

Fig. 16. The impact of feature dimension on classification accuracy based on Sequential Feature Selection.

not work well for the extremes of patient heights can be explained by the nature of the classifier in that there are no near neighbors. We postulate that the reason the Sparse Classifier works better for taller subjects is due to the restriction in bed size. Taller people may not have as much room to move as shorter people and so they have less variation in sleep posture.

4.5. Feature selection

In this section, we examine the effect of feature selection in classification. 32 features are extracted from the pressure image set for classification. It is most certainly the case that some features are redundant or do not have any effect on classification results. We employ Sequential Forward Selection (SFS) to find subsets of features that are most descriptive of the whole feature set [35]. This method is considered a wrapper method, i.e. the feature selection is based on using the classification results themselves and the selection process wraps around the classification.

With this method, the first feature is selected by testing each feature individually in classification. The feature with the highest accuracy performance is chosen first. In the second round of selection, each of the remaining features is used with the first feature in classification. The feature resulting in the highest accuracy is chosen as the second feature in the feature selected subset. This process continues as one feature is added at a time until all of the features are selected. Since the classification always uses previously selected features, redundant features are not selected until the end.

Fig. 16 shows the relationship between number of selected features chosen using SFS and classification accuracy for each of the classifiers. Accuracy generally increases as more features are used for all of the classifiers. There is a sharp increase in accuracy using the Sparse Classifier with both Maximum Sum of Class Coefficients (MSCC) and Minimum Class Residual (MCR) heuristics, from 65% to 78% between 15 features and 20 features. Moreover the three Sparse Classifiers appear to have a threshold at 20 features in the accuracy results, with a smaller rate of increase in accuracy as more features are used. The traditional kNN and Decision Tree show a modest increase of about 10% throughout the whole feature selection process.

An alternative method of selecting features is based on filtering. Each of the features are evaluated based on how well they separate the data into the correct classes. Table 12 shows the order of features ranked by an information gain metric [36]. Information gain describes the reduction in information entropy caused by knowing the value of a feature. Features with high information gain allow better classification. Information gain, IG, is given by

$$IG(A, F) = Entropy(A) - \sum_{f \in F} \frac{|A_f|}{|A|} Entropy(A_f),$$

Table 12
Alternative method of ranking features by Single Feature Selection.

InfoGain	Feat #	Feature	InfoGain	Feat #	Feature
0.887577	17	HipPoint(y)	0.262988	11	Reg7
0.616256	18	HipBox(x)	0.256317	5	Reg1
0.581828	20	HipBox(w)	0.252169	24	ShPoint(x)
0.554651	16	HipPoint(x)	0.234055	32	HipShDist
0.536393	14	Balance	0.215533	23	HipPtoBox
0.497846	19	HipBox(y)	0.200476	29	ShBox(h)
0.47028	22	HipArea	0.196697	3	Per50
0.443133	6	Reg2	0.186926	4	Per75
0.435716	13	Symmetry	0.186884	28	ShBox(w)
0.400952	10	Reg6	0.171033	2	Per25
0.359848	1	Coverage	0.168928	26	ShBox(x)
0.340698	21	HipBox(h)	0.153444	15	DirCurve
0.321448	25	ShPoint(y)	0.143608	30	ShArea
0.318234	9	Reg5	0.126994	12	Reg8
0.302024	27	ShBox(y)	0.12267	8	Reg4
0.277772	31	ShPtoBox	0.117452	7	Reg3

where A_f is the subset of dataset A for which feature F has value f. Entropy is given by

$$Entropy(X) = -\sum_{i=1}^{n} p(x_i) \log_2 p(x_i),$$

where $p(x_i)$ is the probability of sample x_i occurring in the dataset X. The features are chosen one at a time and the classification does not include previously selected features. The disadvantage of this method is that it does not take into account the redundancy in some of the features. In experiments, this method was shown not to be as accurate as the Forward Selection.

It is interesting to note, however, that the highest ranked features are those associated with hip location and bounding box. This can be expected since the different postures do vary greatly in the pressure points of the hip region. It is a strong indicator of side postures versus the supine and prone postures.

5. Conclusion

This work presents a sleep analysis design that monitors sleep posture using a pressure sensitive bedsheet. An application for such a system is to enable caregivers the ability to automatically identify when patients are at risk of developing pressure ulcers or when subjects experience sleep apnea. This work also presents the novel use of relevant features that can be extracted from pressure images, as well as state of the art classification methods. We developed three heuristics for sparse classification, and in our experiments, show that both Maximum Sum of Class Coefficients (MSCC) and Minimum Class Residual (MCR) heuristics produce reliable sleep posture estimation. Through experiments of individual images as well as continuous overnight sequences, we evaluated the effectiveness of this method for sleep posture recognition.

Pressure monitoring systems need not be limited to sleep posture recognition. In nursing home settings, the evaluation of fall risk is a desirable endeavor. Advanced beds are now being developed that can re-distribute support to different regions of the bed [37] and also aid in the heat flow through the bed mattress. Using pressure point monitoring, the goal is to increase the healing speed of patients.

Future work also involves the ability to monitor transitional states as patients move between pre-defined stable classified postures. There are more challenges here because of the large variations in different subjects' motions. 3D model reconstruction of patients from 2D pressure image is another goal that can be accomplished using the results of this research work.

Acknowledgment

The authors would like to thank Medisens Wireless Inc. for their insights and building the hardware.

References

[1] D.J. Buysse, C.F. Reynolds, T.H. Monk, S.R. Berman, D.J. Kupfer, The Pittsburgh sleep quality index: a new instrument for psychiatric practice and research, Psychiatry Research 28 (2) (1989) 193–213.
[2] J. Parish, Sleep-related problems in common medical conditions, Chest Journal 135 (2) (2009) 563–572.
[3] M. Thase, Depression and sleep: pathophysiology and treatment, Dialogues in Clinical Neuroscience 135 (2) (2006) 217–226.
[4] J.B. Lee, Y.H. Park, J.H. Hong, S.H. Lee, K.H. Jung, J.H. Kim, H. Yi, C. Shin, Determining optimal sleep position in patients with positional sleep-disordered breathing using response surface analysis, Journal of Sleep Research 18 (1) (2009) 26–35.
[5] C. Ambrogio, X. Lowman, M. Kuo, J. Malo, A. Prasad, S. Parthasarathy, Sleep and non-invasive ventilation in patients with chronic respiratory insufficiency, Intensive Care Medicine 35 (2013) 306–313.

[6] A. Oksenberg, D. Silverberg, The effect of body posture on sleep-related breathing disorders: facts and therapeutic implications, Sleep Medicine Reviews 2 (3) (2006) 139–162.
[7] C.M. Shapiro, G.M. Devins, M.R. Hussain, ABC of sleep disorders. Sleep problems in patients with medical illness, British Medical Journal 306 (6891) (1993) 1532–1535.
[8] T. Perneger, C. Heliot, A.-C. Rae, F. Borst, J.-M. Gaspoz, Hospital-acquired pressure ulcers: risk factors and use of preventive devices, Archives of Internal Medicine 158 (17) (1998) 1940–1945.
[9] H. Brem, J. Maggi, D. Nierman, L. Rolnitzky, D. Bell, R. Rennert, M. Golinko, A. Yan, C. Lyder, B. Vladeck, High cost of stage IV pressure ulcers, The American Journal of Surgery 200 (2010) 473–477.
[10] K. Nakajima, Y. Matsumoto, T. Tamura, A monitor for posture changes and respiration in bed using real time image sequence analysis, in: Proc. 22nd IEEE Engineering in Medicine and Biology Society, Vol. 1, 2000, pp. 51–54.
[11] W.-H. Liao, C.-M. Yang, Video-based activity and movement pattern analysis in overnight sleep studies, in: 19th International Conference Pattern Recognition, 2008. ICPR 2008, 2008, pp. 1–4.
[12] A. Sadeh, C. Acebo, The role of actigraphy in sleep medicine, Sleep Medicine Reviews 135 (2) (2002) 217–226.
[13] Y. Kishimoto, A. Akahori, K. Oguri, Estimation of sleeping posture for M-Health by a wearable tri-axis accelerometer, in: 3rd IEEE/EMBS International Summer School Medical Devices and Biosensors, 2006, pp. 45–48.
[14] H. Lee, S. Hwang, S. Lee, Y. Lim, K. Park, Estimation of body postures on bed using unconstrained ECG measurements, IEEE Journal Biomedical and Health Informatics 17 (6) (2013) 985–993.
[15] E. Hoque, R.F. Dickerson, J.A. Stankovic, Monitoring body positions and movements during sleep using WISPs, in: Wireless Health 2010, WH'10, 2010, pp. 44–53.
[16] M. Jones, R. Goubran, F. Knoefel, Identifying movement onset times for a bed-based pressure sensor array, in: MeMea IEEE International Workshop Medical Measurement and Applications, 2006, pp. 111–114.
[17] N. Foubert, A. McKee, R. Goubran, F. Knoefel, Lying and sitting posture recognition and transition detection using a pressure sensor array, in: 2012 IEEE International Symposium Medical Measurements and Applications Proceedings, MeMeA, 2012, pp. 1–6.
[18] V. Verhaert, B. Haex, T.D. Wilde, D. Berckmans, M. Vandekerckhove, J. Verbraecken, J.V. Sloten, Unobtrusive assessment of motor patterns during sleep based on mattress indentation measurements, IEEE Transactions on Information Technology in Biomedicine 15 (5) (2011) 787–794.
[19] C. Hsia, K. Liou, A. Aung, V. Foo, W. Huang, J. Biswas, Analysis and comparison of sleeping posture classification methods using pressure sensitive bed system, in: Annual International Conference of the IEEE Engineering in Medicine and Biology Society, 2009. EMBC 2009, 2009, pp. 6131–6134.
[20] H. Ni, B. Abdulrazak, D. Zhang, S. Wu, Unobtrusive sleep posture detection for elder-care in smart home, in: Proceedings of the Aging Friendly Technology for Health and Independence, and 8th International Conference on Smart Homes and Health Telematics, ICOST'10, 2010, pp. 67–75.
[21] Xsensor, http://www.xsensor.com.
[22] VistaMedical, http://www.pressuremapping.com.
[23] W. Xu, Z. Li, M.-C. Huang, N. Amini, M. Sarrafzadeh, eCushion: an eTextile device for sitting posture monitoring, in: IEEE Conference on Body Sensor Networks, BSN, 2011, pp. 194–199.
[24] I. Jolliffe, Principal Component Analysis, in: Springer Series in Statistics, 2013.
[25] R. Yousefi, S. Ostadabbas, M. Faezipour, M. Farshbaf, M. Nourani, L. Tamil, M. Pompeo, Bed posture classification for pressure ulcer prevention, in: Engineering in Medicine and Biology Society, 2011, pp. 7175–7178.
[26] Y. Liu, S.S. Ge, C. Li, Z. You, *k*-NS: a classifier by the distance to the nearest subspace, IEEE Transactions on Neural Networks (2013).
[27] W. Xu, M. Zhang, A. Sawchuk, M. Sarrafzadeh, Co-recognition of human activity and sensor location via compressed sensing in wearable body sensor networks, in: Wearable and Implantable Body Sensor Networks, BSN, 2012, pp. 124–129.
[28] E. Candes, J. Romberg, T. Tao, Robust uncertainty principles: exact signal reconstruction from highly incomplete frequency information, IEEE Transactions on Information Theory 52 (2) (2006) 489–509.
[29] B.K. Natarajan, Sparse approximate solutions to linear systems, SIAM Journal on Computing 24 (2) (1995) 227–234.
[30] L.R. Rabiner, A tutorial on hidden Markov models and selected applications in speech recognition, Proceedings of the IEEE (1989) 257–286.
[31] M. Quwaider, S. Biswas, Body posture identification using hidden Markov model with a wearable sensor network, in: Proceedings of the ICST 3rd International Conference on Body Area Networks, BodyNets'08, 2008, pp. 19:1–19:8.
[32] D.G. Lowe, Distinctive image features from scale-invariant keypoints, International Journal of Computer Vision 60 (2) (2004) 91–110.
[33] C. Idzikowski, Beating Insomnia: How to Get a Good Night's Sleep, Gill & MacMillan, 2003.
[34] CVX Research Inc., CVX: Matlab software for disciplined convex programming, version 2.0, August 2012. http://cvxr.com/cvx.
[35] G.H. John, R. Kohavi, K. Pfleger, Irrelevant features and the subset selection problem, in: Machine Learning: Procs. 11th International Conference, Morgan Kaufmann, 1994, pp. 121–129.
[36] T.M. Cover, J.A. Thomas, Elements of Information Theory, Wiley-Interscience, New York, NY, USA, 1991.
[37] Hillrom, http://www.hill-rom.com.